Journal of Biomechanics 88 (2019) 130–137

Contents lists available at ScienceDirect

Journal of Biomechanics

journal homepage: www.elsevier.com/locate/jbiomech
www.JBiomech.com

Study of bovine sperm motility in shear-thinning viscoelastic fluids

Toru Hyakutake [a,*], Koichi Sato [b], Kenta Sugita [b]

[a] Faculty of Engineering, Yokohama National University, 79-5, Hodogaya, Yokohama 240-8501, Japan
[b] Graduate School of Engineering, Yokohama National University, 79-5, Hodogaya, Yokohama 240-8501, Japan

ARTICLE INFO

Article history:
Accepted 21 March 2019

Keywords:
Bovine sperm
Shear-thinning viscoelastic fluid
Flagella
Thrust efficiency

ABSTRACT

To elucidate the process whereby sperm arrive at an egg in the female reproductive organs, it is essential to investigate how rheological properties of the fluid around mammalian spermatozoa affect their motility. We examined the motility and flagellar waveform of bovine sperm swimming in a fluid with similar rheological properties as mammalian cervical mucus. The results indicated that the surrounding rheological properties largely affected the flagellar waveform of mammalian spermatozoa; in particular, shear-thinning viscoelastic fluid increased the progressive motility of the sperm. To investigate the influence of flagellar waveform on sperm motility in more detail, the waveform was expressed as a function and the progressive thrust of the sperm was calculated based on the empirical resistive force theory. The results of this study showed that the progressive thrust increased with the curvature of the flagellar tip. Moreover, we calculated the thrust efficiency of motile sperm. Results showed that the thrust efficiency in shear-thinning viscoelastic fluids was larger than that in Newtonian fluids, regardless of viscosity. This suggests that motile sperm in cervical mucus move efficiently by means of a motion mechanism that is suited to their surrounding environment.

1. Introduction

For mammals, successful internal fertilization requires a progressively motile spermatozoon for approaching an egg. The numerous sperm cells ejaculated in the vagina move forward in the uterine tube via the cervical canal and body of the uterus. To reach an egg in the uterine tube, mammalian sperm progress through the active motion of a slender flagellum. This considerably long journey required for a mammalian spermatozoon to meet an egg in the female reproductive organs has not yet been clarified sufficiently owing to the complexity of the phenomenon. Several characteristic circumstances influence the journey of sperm. Cervical mucus is a highly viscous fluid, and its viscosity depends on the shear rate (Lai et al., 2007). The viscous properties vary during the female menstrual cycle (Wolf et al., 1977b) and differ considerably among individuals (Tam et al., 1980). In these rheological circumstances, a sperm moves along a microgroove on the uterine tubal surface against the flow due to tubal peristalsis (Mullins and Saacke, 1989; Tung et al., 2015). In addition, a change in sperm motion, called hyperactivation, may occur via signal transduction through a medium of calcium ions en route to the egg (Katz et al., 1989; Yanagimachi, 1970). Therefore, sperm motility is influenced significantly by factors such as fluid dynamics, morphology and chemical composition. Given this background, we focus herein on how the fluid rheological properties of cervical mucus affect sperm motility.

Mammalian cervical mucus possesses quite characteristic viscous properties (Eliezer, 1974; Litt et al., 1976). Wolf et al. (1977a) found that the mucus in the uterine tube is a viscoelastic fluid that contains gelatinous materials and macromolecules. Tam et al. (1980) measured the viscoelastic properties of human and bovine cervical mucus and reported nonlinearity of the cervical mucus. Lai et al. (2007) measured the viscosity of fresh human cervical mucus samples as a function of shear rate; they indicated that the mucus was a non-Newtonian fluid whose viscosity exceeded that of water by two to three orders of magnitude. Several studies have reported the motion characteristics of mammalian sperm in a highly viscoelastic fluid. Rikmenspoel (1984) observed experimentally the motility of bovine sperm in methylcellulose with viscosities of 0.001–4 Pa s. Smith et al. (2009) used methylcellulose to conduct a detailed investigation of human sperm motility and the flagellar waveform in fluids of low and high viscosity. Hyakutake et al. (2015a,b) used polyvinylpyrrolidone and methylcellulose to investigate the effect of viscosity and non-Newtonian fluid on the motion characteristics of bovine sperm. These studies clarified that the surrounding rheological properties affected mammalian sperm motility. However, the

* Corresponding author.
E-mail address: hyaku@ynu.ac.jp (T. Hyakutake).

https://doi.org/10.1016/j.jbiomech.2019.03.035
0021-9290/

molecular weight of the macromolecules that construct the cervical mucus is larger than that of the polyvinylpyrrolidone and methylcellulose used in existing studies. Therefore, to appropriately estimate the motility of mammalian sperm in female reproductive organs, investigating sperm motility for the rheological conditions approaching actual cervical mucus is essential.

Given this background, we investigated the motion characteristics of bovine sperm swimming in a medium with the rheological properties which are close to those of mammalian cervical mucus. We used polyacrylamide (PAA) solution as swimming medium, which possesses shear-thinning and viscoelastic properties. For comparison, we also investigated the sperm motion and flagellar waveform in Newtonian fluids with low and high viscosities to clarify the effects of shear-thinning and viscoelastic properties. Additionally, the thrust efficiency of motile sperm was calculated from sperm velocity and the time variation of flagellar waveform. The obtained experimental results will be useful in clarifying the mechanics of mammalian sperm motility under their actual environmental conditions. Furthermore, the results will provide valuable information for the reproduction industry in the field of animal husbandry to further assisted reproductive technology (Cho et al., 2003; Chen et al., 2011; Hyakutake et al., 2009; Knowlton et al., 2015; Matsuura et al., 2012; Rappa et al., 2016; Sano et al., 2010; Schuster et al., 2003; Seo et al., 2007).

2. Materials and methods

In this study, we used Japanese cattle semen (Fukuteruyoshi; Animal Genetics Japan Co., Ltd., Suzuka, Japan) that had been cryopreserved in 0.5-ml straws. First, the semen was thawed and added to a Tris-citric acid-glucose solution to sustain the sperm motility and extend observation time. Next, to facilitate observations, bovine semen was separated into sperm and seminal plasma using a centrifugal separator for a duration of 10 min. The separated sperm was diluted with phosphate-buffered saline and then added to PAA and polyvinylpyrrolidone (PVP) solutions (Wako Pure Chemical Industries, Ltd., Osaka, Japan) to change the rheological properties of the sperm solution. The PAA and PVP had molecular weights of 18,000 and 360 kDa, respectively. PAA and PVP solutions were produced by dissolving powdered reagents in pure water while simultaneously stirring the solution. This suspension was heated in a water bath at 38.5 °C, and during the observation period the temperature of the suspension was maintained using a thermoplate. The suspension was placed on a hole slide glass and covered with a coverslip. The hole slide glass used in this study has a chamber with a diameter of 14–15 mm and a depth of 0.6 mm. The motion of the sperms away from the wall and the interface were also observed. Sperm motion was observed using an optical microscope (IX71; Olympus, Tokyo, Japan) and images were obtained using a CCD camera (K-II; Kato Koken, Isehara, Japan). A rheometer (ARES-G2; TA Instruments, New Castle, DE, USA) was used to measure the viscoelastic properties of the PAA and PVP solutions at 38.5 °C. In this study, we selected three PAA concentrations (0.2%, 0.5% and 0.8%) and two PVP concentrations (10% and 15%). All sperm experiments were conducted using the solutions produced from the same preparation.

Sperm motion was observed under a microscope and images were obtained at 100 fps using a high-speed camera. For image analysis, particle-tracking velocimetry was applied using the DIPP-Motion V fluid analysis software (Ditect Co., Ltd., Tokyo, Japan). Sperm trajectories were obtained by marking the sperm heads in the images. The analysis time is one second per sample. Based on the trajectories, two types of velocity were obtained using MATLAB (MathWorks, Natick, MA, USA). First, the curvilinear velocity (VCL) was calculated by averaging the velocities determined from the change in sperm position between each pair of successive images. Second, the straight-line velocity (VSL) was calculated using the distance between sperm position in the first and last frames. Regarding the velocity average path (VAP), hardly any difference was observed between VSL and VAP owing to the short analysis time. Therefore, the results related to VAP were omitted in this article. Regarding sperm motility, the beat frequency was measured directly from images obtained for one second. Moreover, the time variation of flagellar shape was quantified by conducting image thresholding using DIPP-Motion V and was compared for several typical sperm samples.

3. Results

First, we investigated the rheological properties of swimming media. Fig. 1 shows the relationship between shear rate and viscosity for the three PAA concentrations. The range of shear rate is 10^{-2}–10^{3} s^{-1}. The viscosity of the PAA solution exceeded that of water (0.67 mPa s at 38.5 °C) by two to four orders of magnitude. Additionally, the viscosity decreased with shear rate. Therefore, the PAA solutions were non-Newtonian fluid, particularly shear-thinning fluids. By contrast, the viscosities of the diluted solution and the 10% and 15% PVP solutions (0.80, 99 and 450 mPa s, respectively) were almost constant regardless of the shear rate. Therefore, the diluted solution and the PVP solutions were simple Newtonian fluids.

For comparison, the typical viscosity of the non-ovulatory cervical mucus of humans is also shown in Fig. 1. This data is an average of 13 samples. The rheological properties of cervical mucus are closest to those of 0.5% PAA. Actually, the viscosity of cervical mucus varies according to the female menstrual cycle and differs considerably among individuals. Therefore, it is important to investigate sperm motility in shear-thinning fluids with wide range of viscous properties. Additionally, to estimate the shear-thinning fluid properties of PAA solution quantitatively, experimental data measured by a rheometer were fitted using the Carreau model. The Carreau model is defined as

$$\mu = \mu_\infty - (\mu_\infty - \mu_0)\left[1 + (\Gamma\dot{\gamma})^2\right]^{\frac{n-1}{2}} \quad (1)$$

where μ_0 and μ_∞ are the viscosities at zero shear rate and infinite shear rate, respectively, Γ is the time constant, n is the power index

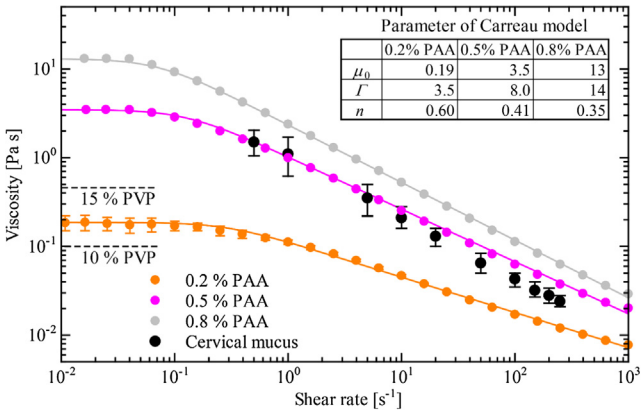

Fig. 1. Relationships between shear rate and viscosity for 0.2%, 0.5% and 0.8% PAA, which are shear-thinning fluids. The measured data are fitting using the Carreau model (solid lines). The fitting parameters μ_0, Γ, and n are shown in the inset table, where μ_0 is viscosity at zero shear rate, Γ is time constant and n is power index. For comparison, measured data for the viscosity of the non-ovulatory cervical mucus of humans are also shown (Lai et al., 2007). Additionally, the viscosities of 10% and 15% PVP, which are Newtonian fluids, are shown (dotted lines).

and $\dot{\gamma}$ is the shear rate. Γ and n were obtained using the least squares method, wherein we defined μ_0 as the viscosity for the smallest shear rate and μ_∞ as 0. The results are given in the table in Fig. 1.

Fig. 2 shows the results of the dynamic viscoelastic properties of swimming media. We measured the storage modulus (G′) and loss modulus (G″) for the three PAA concentrations. As the angular frequency was increased, both moduli increased. The increase in the PAA concentration brought about increase in the two moduli. At 25 rad/s, the values of the loss factor tanθ for 0.2%, 0.5% and 0.8% PAA were 0.839, 0.556 and 0.474, respectively. Under the assumption of the Maxwell model, we obtained the relaxation time from the point of intersection between G′ and G″. Thus, the relaxation times for 0.2%, 0.5% and 0.8% PAA were 0.063, 1.0 and 4.0, respectively.

Fig. 3 shows the relationship between VCL and VSL obtained from videos of sperm motion for each reagent. The lower figure is enlarged view of low sperm velocity area of upper figure. The experiments were conducted in the stationary fluid. It is clear that the sperm in the diluted solution moves faster than those in the other reagents. As the reagent concentration was increased, both sperm velocities decreased. The average values of VCL and VSL are summarized in Fig. 4(a) and (b), respectively, where the horizontal axes represent viscosity at zero shear rate and the error bars are the standard deviations. With PVP solution, increasing the viscosity of the fluid surrounding the sperm dramatically decreased VCL and VSL. By contrast, with PAA solution, increasing the viscosity decreased these sperm velocities far more gradually than with PVP solution. Next, the linearity of a sperm trajectory (LIN), which is defined as the ratio of VSL to VCL, was calculated to estimate the sperm motility. Fig. 4(c) compares LIN for each reagent. With PVP solution, LIN decreased with viscosity. By contrast, with PAA solution, LIN increased with viscosity. Additionally, we obtained the frequency of a sperm trajectory, which corresponds to the frequency of the sperm flagellum motion. Fig. 4(d) shows the relationship between viscosity at zero shear rate and frequency. The tendency is similar to that of the sperm velocities: with PVP solution, the frequency decreased appreciably with viscosity; with PAA solution, the frequency decreased gradually with viscosity.

Next, we investigated how the surrounding rheological properties influenced the sperm flagellar waveform. Fig. 5(a)–(c) illustrate snap shots of three typical flagellar waveforms in samples of each reagent, where (a), (b) and (c) indicate 0.8% PAA (Shear-thinning viscoelastic fluid), the diluted solution (low-viscosity Newtonian fluid) and 15% PVP (high-viscosity Newtonian fluid), respectively. The three images on the right show the time variation of the flagellar waveforms at intervals of 10 ms, where the black bars represent 5 μm. From these figures, the flagellar waveform in the diluted solution was close to a sinusoidal wave. By contrast, the curvature of the flagellar waveform in 0.8% PAA increased away from the flagellar root. In 15% PVP, the flagellar amplitude decreased overall. Of the three cases, the wavelength of the motion was longest in the diluted solution.

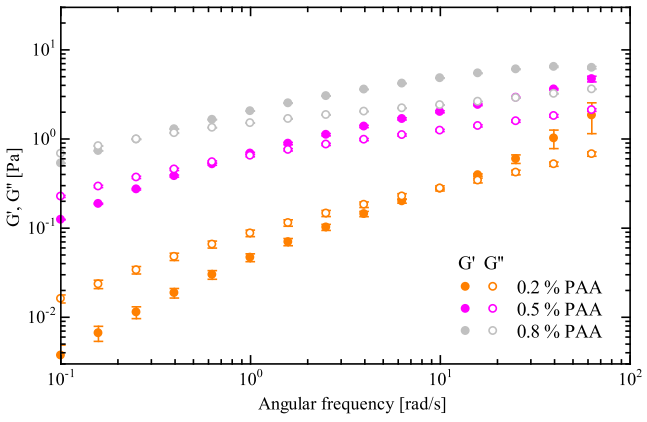

Fig. 2. Relationships between angular frequency and storage and loss moduli (G′ and G″) for 0.2%, 0.5% and 0.8% PAA.

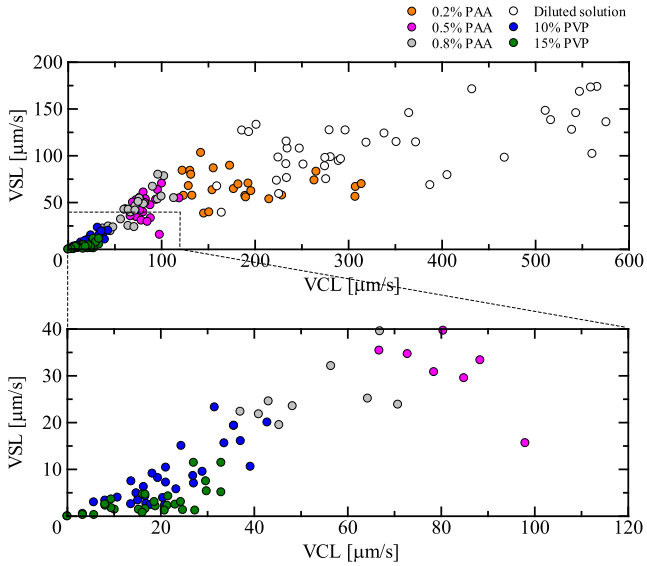

Fig. 3. Relationship between curvilinear velocity (VCL) and straight-line velocity (VSL) obtained from videos of sperm motion for each reagent. The lower figure is enlarged view of low sperm velocity area of upper figure. The sample sizes of 0.2%, 0.5% and 0.8% PAA are 25, 24 and 22, respectively. The sample sizes of the diluted solution and 10% and 15% PVP are, 41, 29 and 29, respectively.

The time variations of these flagellar waveforms obtained from the videos were quantified by discretising the flagellar waveforms at 20 nodes and assigning them coordinate data. Fig. 6 shows the flagellar curvature at three time steps, where (a) is 0.8% PAA, (b) is the diluted solution and (c) is 15% PVP. The horizontal axes indicate the normalized distance from the flagellar root. For 0.8% PAA, the flagellar curvature was almost zero at the root, whereas it increased rapidly with fluctuations away from the root. As time progressed, the peak curvature shifted right while increasing. By contrast, for the dilute solution, the curvature shifted right while fluctuating, but it did not increase away from the root. For 15% PVP, the shifted distance was small and the increment of the curvature was small compared with 0.8% PAA.

The thrust efficiency of the sperm cell swimming in each reagent was calculated from the time-variation data of the flagellar waveform. The thrust efficiency is defined as

$$\eta = \frac{\bar{Z}}{\bar{W}} V \tag{2}$$

where $\bar{Z}$ [N] is the time-averaged thrust of the sperm head, $\bar{W}$ [W] is time-averaged power generated by the sperm flagellum and V [m/s] is the VSL. Based on a simple assumption of a spherical sperm head, the thrust was calculated using the Stokes approximation as follows.

$$\bar{Z} = \frac{1}{T}\sum_{t=0}^{T} \quad Z = \frac{1}{T}\sum_{t=0}^{T} 6\pi\mu a U \tag{3}$$

where T is time of one beat and U is the instantaneous velocity of the sperm head. Morphologically, the diameter of the flagellum decreases away from the root. To calculate the power generated by the sperm flagellum, we assumed that the diameters of the flag-

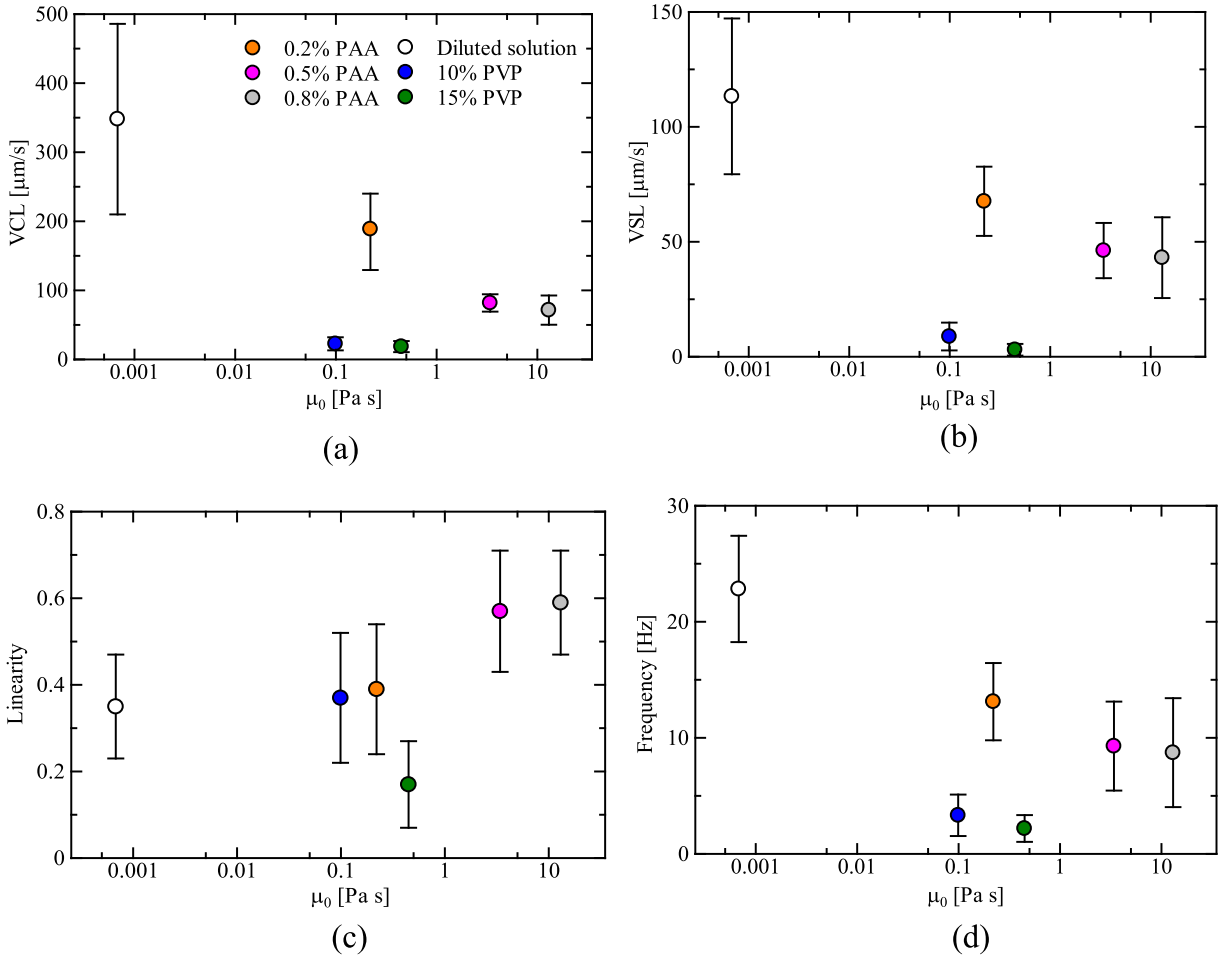

Fig. 4. (a) Relationship between VCL and viscosity at zero shear rate. (b) Relationship between VSL and viscosity at zero shear rate. (c) Relationship between linearity (LIN) and viscosity at zero shear rate. (d) Relationship between frequency and viscosity at zero shear rate.

ellum at $s = 0$ and 1 in Fig. 6 were 2.0 and 1.0 μm, respectively and linear interpolation was conducted between $s = 0$ and 1. With Newtonian fluid, the drag acting on the flagellum was calculated using the resistive force theory (Gray and Hancock, 1955; Lighthill, 1976). Moreover, to calculate the drag acting on the slender flagellum in shear-thinning fluid, we introduced the following empirical drag-coefficient correction factor proposed by Riley and Lauga (2017):

$$R_E = \left\{ 1 + 0.317 \left[\frac{(1-n)\Gamma|\boldsymbol{u}|}{d_s} \right]^{0.692} \right\}^{-1} \tag{4}$$

where $d_s = \sqrt[3]{3Ld^2}$ is the equivalent sphere diameter, L is the flagellar length and d is the flagellar diameter. For n and Γ, we applied the values obtained for each reagent using the rheometer (Fig. 1). Therefore, the tangential and normal drag coefficients in the shear-thinning fluids are corrected as follows:

$$C_L^{'} = R_E C_L, \quad C_N^{'} = R_E C_N \tag{5}$$

where C_L and C_N are the tangential and normal drag coefficients, respectively, based on the resistive force theory. Additionally, in the case of the thrust of the sperm head in the shear-thinning fluid, we applied the empirical drag-coefficient correction factor of Eq. (4), wherein we assumed d_s as the diameter of the sperm head, i.e., $2a$. Consequently, we can modify the thrust of the sperm head as $Z' = R_E Z$.

Fig. 7(a)–(c) show the sample mean of the time-averaged thrust of the sperm head, the time-averaged power generated by the sperm flagellum and the thrust efficiency, respectively. With both PAA and PVP solutions, the time-averaged thrust increased linearly with viscosity. By contrast, for the time-averaged power, there was discrepancy between PAA and PVP solutions. As a result, the thrust efficiency with PAA solution was roughly twice that with PVP solution. Increasing the viscosity had little influence on the thrust efficiency.

Finally, we investigated the influence of the flagellar waveform on progressive motility. We applied the flagellar-waveform model proposed by Montenegro-Johnson et al. (2012), wherein the tangent angle is given as

$$\psi(s,t) = Cs\cos(ks - t) \tag{6}$$

where C and k are parameters relating to the flagellar amplitude and wave number, respectively. Fig. 8(a) shows several flagellar waveforms for various values of C with $k = 2.5$. Increasing the value of C increases the curvature of the flagellar tip. The flagellar waveform for $C = 1.2\pi$ was quite similar to that in the 0.8% PAA (Fig. 5(a)). For small C, by contrast, the waveform was close to that in the 15% PVP (Fig. 5(c)). From the time variation of this flagellar-waveform model, we calculated the drag acting on the flagellum by applying Eq. (5). We estimated the progressive thrust F_x as counterforce of the force acting on the flagellum. Fig. 8(b) shows the relationship between thrust F_x and parameter C for diluted and the three PAA solutions, where F_x was normalized by the thrust at $n = 1$ and

(a) 0.8% PAA

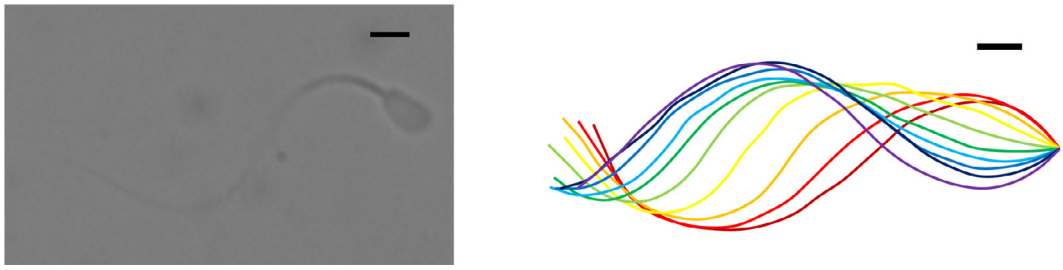

(b) Diluted solution

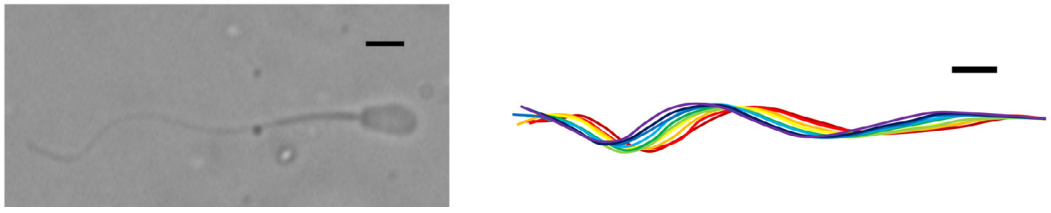

(c) 15% PVP

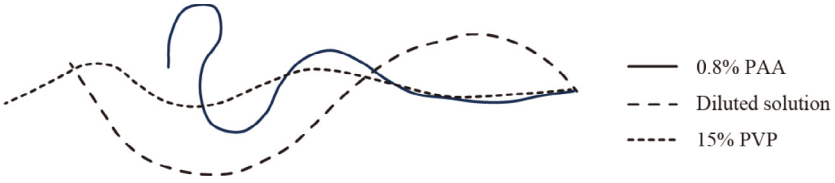

(d) Superposition of flagellar waveform for three cases

Fig. 5. Left: snapshots of typical flagellar waveforms, where (a), (b) and (c) indicate 0.8% PAA, diluted solution and 15% PVP, respectively. Right: time variations of flagellar waveforms at 10-ms intervals (black bars represent 5 μm), (d) Superposition of flagellar waveform for three cases.

$C = \pi$. From this figure, F_x increased with C. As shear-thinning fluid property increased, i.e., as n decreased and λ increased, F_x decreased.

4. Discussion

In the past decade, several studies have focused on how the rheological properties of the surrounding fluid affect flagellar swimmers. The viscosity of cervical mucus exceeds that of water by two to four orders of magnitude and the mucus has viscoelastic properties. The relationship between viscosity and shear rate indicates that the mucus is a non-Newtonian fluid, in particular a shear-thinning fluid. Therefore, for mammalian spermatozoa that perform internal fertilization, it is important to investigate how the rheological properties of the cervical mucus influence the motility of swimming sperm. The present study observed the motion of bovine sperm swimming in fluid whose rheological properties were close to those of actual cervical mucus. The results indicated that the surrounding rheological properties largely affected the flagellar waveform of mammalian spermatozoa; in particular, shear-thinning viscoelastic fluid increased the progressive motility of the sperm. It is valuable to have achieved experiments in a surrounding fluid whose properties are close to those of actual cervical mucus.

In the present study, as well as making observations in shear-thinning viscoelastic fluids, we also investigated sperm motility in Newtonian fluids for comparison. The concentrations of the prepared Newtonian fluids (PVP solutions) were 0% (diluted solution), 10% and 15% and their viscosities were 0.80, 99 and 450 Pa s, respectively. In agreement with previous studies with the diluted solution, the experiment results with low-viscosity Newtonian fluid indicated that sperm moved forward in a zigzag pattern, and the flagellar waveform was nearly sinusoidal (Fig. 5(b)). By

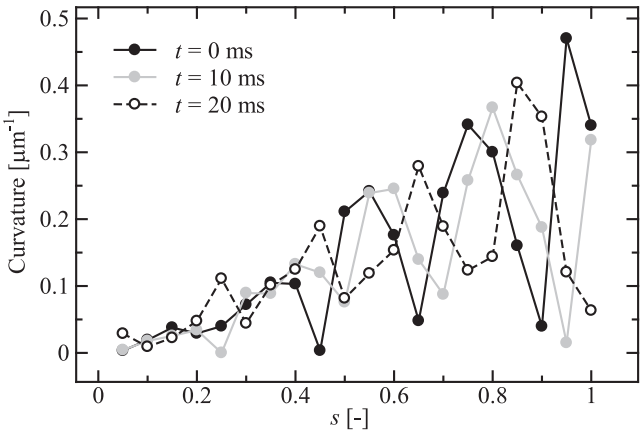

(a) 0.8% PAA

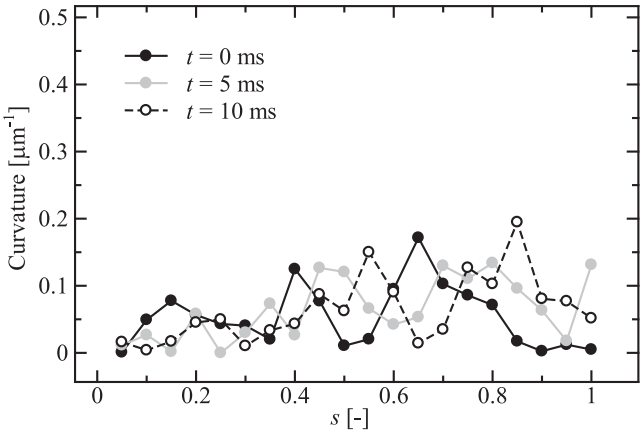

(b) Diluted solution

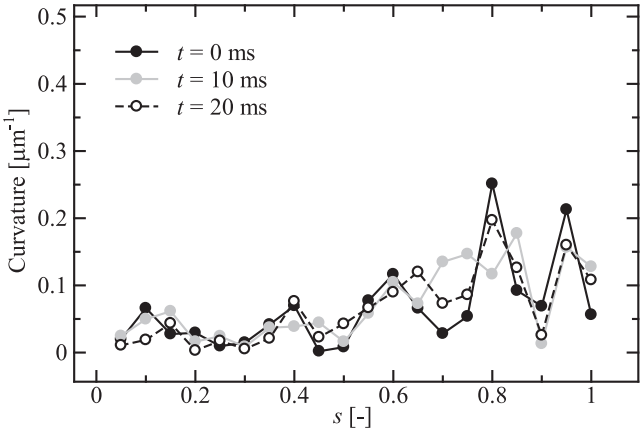

(c) 15% PVP

Fig. 6. Flagellar curvature at three time steps, where (a) is 0.8% PAA, (b) is diluted solution and (c) is 15% PVP. The horizontal axes indicate normalized distance from flagellar root.

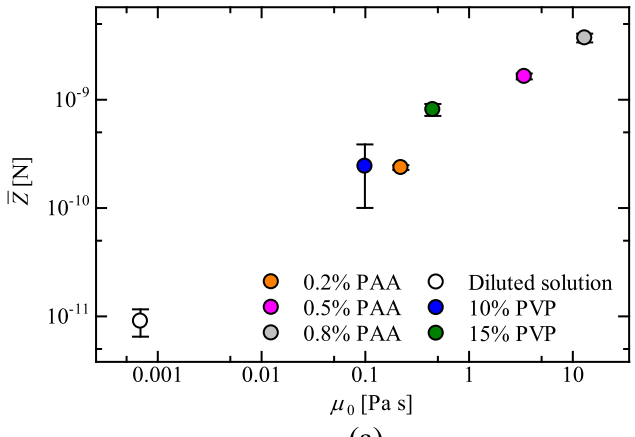

(a)

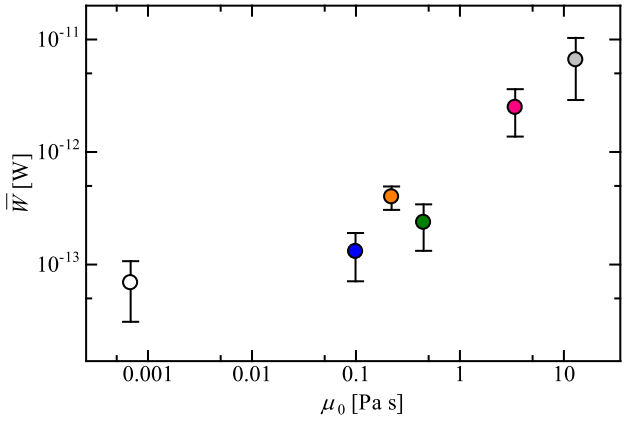

(b)

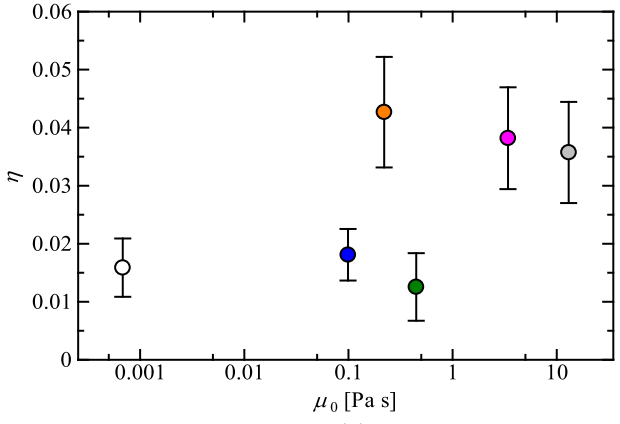

(c)

Fig. 7. (a) Time-averaged thrust of sperm head for each reagent. (b) Time-averaged power generated by sperm flagellum. (c) Thrust efficiency.

contrast, in the high-viscosity Newtonian fluid, the sperm velocity decreased drastically, and the linearity also decreased. The flagellar waveform differed from that in the shear-thinning viscoelastic fluids, and the amplitude was small from the root to the tip of the flagellum (Fig. 5(c)). These results suggest that it was only the increased viscosity that brought about the loss of progressive motility, which relates directly to fertility. The existence of shear-thinning viscoelastic behavior around the flagellum avoids rapid decrease in straight-line velocity, thereby increasing the progressive motility. Consequently, we infer that the sperm flagella execute the correct motion for fertility according to the rheological characteristics in the female reproductive organs.

To investigate in more detail how the flagellar waveform influences sperm motility, the waveform was expressed as a mathematical function (Montenegro-Johnson et al., 2012), and the progressive thrust of the sperm was calculated based on the empirical resistive force theory in shear-thinning fluids (Riley and Lauga,

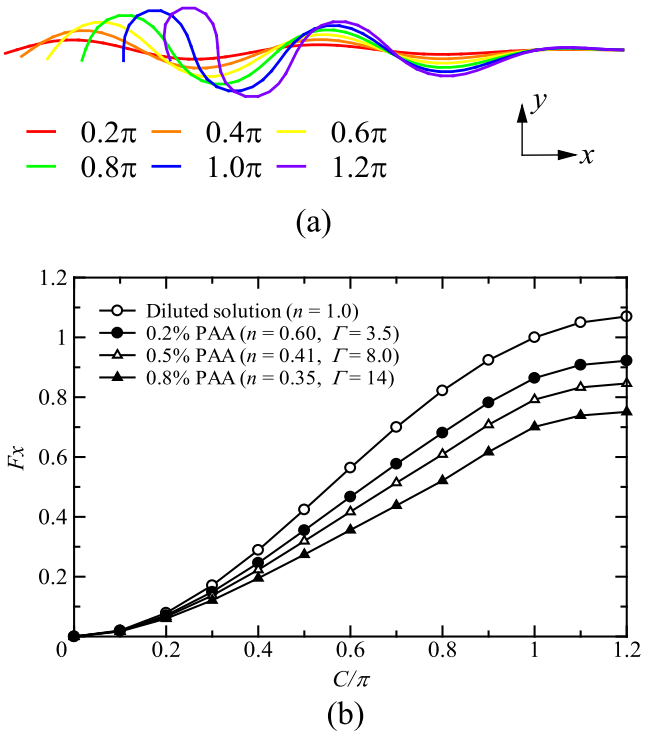

Fig. 8. (a) Several flagellar waveforms modeled by Eq. (6), varying parameter C with $k = 2.5$. (b) Relationship between thrust F_x and parameter C for diluted and three PAA solutions, where F_x is normalized by the thrust at $n = 1$ and $C = \pi$.

2017). The results showed that the progressive thrust increased with the curvature of the flagellar tip, as shown in Fig. 8(b). Some factors determine the flagellar waveform, i.e., microtubule sliding driven by dynein, the elastic stiffness of the flagellum, and the surrounding rheological property. Consequently, the characteristic waveform in shear-thinning fluids leads to increased linearity. Because the diameter of the sperm head is greater than that of the flagellum, the speed and amplitude of the head decrease further. This also contributes to the increased linearity. Comparing the typical waveforms of 0.8% PAA and 15% PVP obtained from the experimental videos (Fig. 5(a) and (c)) with those in Fig. 8(a) expressed as a function, the values of the parameter C for 0.8% PAA and 15% PVP are approximately 1.2π and 0.4π, respectively. From Fig. 8(b), therefore, the values of F_x for 0.8% PAA and 15% PVP are estimated to be approximately 0.75 and 0.30, respectively. This result explains why the linearity of 0.8% PAA decreased by about 70% in comparison with that of 15% PVP, as shown in Fig. 4(d). Moreover, we calculated the thrust efficiency of motile sperm (Fig. 7(c)). The results showed that the thrust efficiency in the shear-thinning viscoelastic fluids was roughly twice that in the Newtonian fluids including the diluted solution. This suggests that motile sperm in cervical mucus move efficiently by means of a motion mechanism that is suited to their environment.

Smith et al. (2009) reported that the flagellar waveform of human sperm changes according to the surrounding rheological properties. They used methylcellulose solution as a surrounding fluid with adjustable viscosity, the maximum viscosity of which was 1.6 Pa s. Hyakutake et al. (2015b) used methylcellulose to investigate bovine sperm motility and noted increased linearity in non-Newtonian fluid. In the present study, using PAA (whose molecular weight is much larger than that of methylcellulose) allowed experiments to be performed in fluid whose rheological properties were almost the same as those of actual bovine cervical mucus. Furthermore, Tung et al. (2017) used PAA to mimic the physical properties of bovine cervical mucus during the fertile period of the hormonal cycle and investigated collective swimming of bovine sperm. The molecule weight of PAA used by Tung et al. (2017) was 5000–6000 kDa, whose rheological properties were close to that used in this study. The viscoelastic properties can be estimated using the loss factor $\tan\theta$ as the ratio of the loss modulus G'' to the storage modulus G'. Wolf et al. (1977a) investigated the rheological characteristics of bovine cervical mucus, and the loss factor was approximately 0.5 at 10 rad/s. Tam et al. (1980) measured the viscoelastic properties of bovine cervical mucus, and at 30 rad/s the loss factor was 0.01–0.4; this relatively wide range was due to individual differences. We also measured the dynamic viscoelastic properties of PAA using a rheometer. At 25 rad/s, the values of the loss factor $\tan\theta$ for 0.2%, 0.5% and 0.8% PAA were 0.839, 0.556 and 0.474, respectively (Fig. 2). In the experiment of Smith et al. (2009), the loss factor of methylcellulose used was 1.88 at the highest viscosity. Therefore, the viscoelastic properties of the reagent used in the present study are considerably closer to those of actual bovine cervical mucus by comparison with the viscoelastic properties of the reagent used in existed studies.

We obtained the relaxation time from the point of intersection between G' and G'' under the assumption of the Maxwell model. Thus, the relaxation times for 0.2%, 0.5% and 0.8% PAA were 0.063, 1.0 and 4.0, respectively. Tam et al. (1980) reported that the relaxation time of bovine cervical mucus was 0.5–53 s. Therefore, the relaxation times of 0.5% and 0.8% PAA were within the range of actual cervical mucus. As shown in Fig. 4(e), the flagellar frequencies of bovine sperm in 0.5% and 0.8% PAA were 9.3 and 8.7 Hz, respectively. From the relaxation time λ and the frequency ω, the Deborah number, which is defined as $De = \lambda\omega$, is calculated to be 9.3–35, values that are much greater than one. In high Deborah number, it is considered that the viscosity remains smaller while moving the flagellum due to the shear-thinning effect. Thus, the characteristic flagellar waveform was formed, which increased the progressive motility. Lauga (2009) mentioned that high Deborah numbers play an important role in the motility of mammalian sperm swimming in cervical mucus. Therefore, the present study represents an important experiment using high Deborah numbers that were closer to those of the actual environment compared with the Deborah numbers used in previous studies. In the future, it will be important to study in more detail the interaction between viscoelasticity and the flagellar mechanics of spermatozoa.

5. Conclusions

In the present study in focusing on the shear-thinning viscoelastic behavior that is a characteristic rheological property of mammalian cervical mucus, the motility of bovine sperm swimming in shear-thinning viscoelastic fluids closely resembling actual cervical mucus was investigated. The experimental results indicated differing sperm motility according to the rheological properties of the fluid surrounding the spermatozoa. Shear-thinning viscoelastic fluid increased the linearity. Furthermore, the thrust efficiency of motile sperm was calculated by applying the empirical resistive force theory for the shear-thinning fluids. The results showed that the thrust efficiency was influenced far more by the shear-thinning viscoelastic behavior than by viscosity. Calculations using a flagellar-waveform model suggested that the increased curvature of the flagellar tip enhanced the progressive motile capacity. These results will help us to understand properly the mechanics of sperm motility in actual female reproductive organs.

Conflict of interest statement

The authors confirmed that there are no known conflicts of interest associated with this publication and there has been no sig-

nificant financial support for this work that could have influenced its outcome.

Acknowledgement

This research was supported by a Grant-in-Aid for Challenging Exploratory Research (No. 26560204) from the Japan Society for the Promotion of Science.

References

Chen, Y.A. et al., 2011. Analysis of sperm concentration and motility in a microfluidic device. Microfluid Nanofluidics 10, 59–67.
Cho, B.S. et al., 2003. Passively driven integrated microfluidic system for separation of motile sperm. Anal. Chem. 75, 1671–1675.
Eliezer, N., 1974. Viscoelastic properties of mucus. Biorheology 11, 61–68.
Gray, J., Hancock, G.J., 1955. The propulsion of sea-urchin spermatozoa. J. Exp. Biol. 32, 802–814.
Hyakutake, T., Hashimoto, Y., Yanase, S., Matsuura, K., Naruse, K., 2009. Application of a numerical simulation to improve the separation efficiency of a sperm sorter. Biomed. Microdev. 11, 25–33.
Hyakutake, T., Suzuki, H., Yamamoto, S., 2015a. Effect of viscosity on motion characteristics of bovine sperm. J. Abmech. 4, 63–70.
Hyakutake, T., Suzuki, H., Yamamoto, S., 2015b. Effect of non-Newtonian fluid properties on bovine sperm motility. J. Biomech. 48, 2941–2947.
Katz, D.F., Drobnis, E.Z., Overstreet, J.W., 1989. Factors regulating mammalian sperm migration through the female reproductive tract and oocyte vestments. Gamete Res. 22, 443–469.
Knowlton, S.M., Sadasivam, M., Tasoglu, S., 2015. Microfluidics for sperm research. Trends Biotechnol. 33, 221–229.
Lai, S.K. et al., 2007. Rapid transport of large polymeric nanoparticles in fresh undiluted human mucus. PNAS 104, 1482–1487.
Lauga, E., 2009. Life at high Deborah number. Europhys. Lett. 86, 64001.
Lighthill, J., 1976. Flagellar hydrodynamics. SIAM Rev. 18, 161–230.
Litt, M., Khan, M.A., Wolf, D.P., 1976. Mucus rheology: relation to structure and function. Biorheology 13, 37–48.
Matsuura, K. et al., 2012. Screening of sperm velocity by fluid mechanical characteristics of a cyclo-olefin polymer microfluidic sperm-sorting device. Reprod. Biomed. Online 24, 109–115.
Montenegro-Johnson, T.D., Smith, A.A., Smith, D.J., Loghin, D., Blake, J.R., 2012. Modelling the fluid mechanics of cilia and flagella in reproduction and development. Europ. Phys. J. E Soft Matter 35, 111.
Mullins, K.J., Saacke, R.G., 1989. Study of the functional anatomy of bovine cervical mucosa with special reference to mucus secretion and sperm transport. Anat. Rec. 225, 106–117.
Rappa, K.L. et al., 2016. Sperm processing for advanced reproductive technologies: where are we today? Biotechnol. Adv. 34, 578–587.
Rikmenspoel, R., 1984. Movements and active moments of bull sperm flagella as a function of temperature and viscosity. J. Exp. Biol. 108, 205–230.
Riley, E.E., Lauga, E., 2017. Empirical resistive-force theory for slender biological filaments in shear-thinning fluids. Phys. Rev. E 95, 062416.
Sano, H., Matsuura, K., Naruse, K., Funahashi, H., 2010. Application of a microfluidic sperm sorter to the in-vitro fertilization of porcine oocytes reduced the incidence of polyspermic penetration. Theriogenology 74, 863–870.
Schuster, T.G., Cho, B., Keller, L.M., Takayama, S., Smith, G.D., 2003. Isolation of motile spermatozoa from semen samples using microfluidics. Reprod. Biomed. Online 7, 75–81.
Seo, D.-B., Agca, Y., Feng, Z.C., Critser, J.K., 2007. Development of sorting, aligning, and orienting motile sperm using microfluidic device operated by hydrostatic pressure. Microfluidics Nanofluidics 3, 561–570.
Smith, D.J., Gaffney, E.A., Gadêlha, H., Kapur, N., Kirkman-Brown, J.C., 2009. Bend propagation in the flagella of migrating human sperm and its modulation by viscosity. Cell Motil. Cytoskelet. 66, 220–236.
Tam, P.Y., Katz, D.F., Berger, S.A., 1980. Non-linear viscoelastic properties of cervical mucus. Biorheology 17, 465–478.
Tung, C.K. et al., 2015. Microgrooves and fluid flows provide preferential passageways for sperm over pathogen Tritrichomonas foetus. PNAS 112, 5431–5436.
Tung, C.K. et al., 2017. Fluid viscoelasticity promotes collective swimming of sperm. Sci. Rep. 7, 3152.
Wolf, D.P., Blasco, L., Khan, M.A., Litt, M., 1977a. Human cervical mucus. I. Rheologic characteristics. Fert. Steril. 28, 41–46.
Wolf, D.P., Blasco, L., Khan, M.A., Litt, M., 1977b. Human cervical mucus. II. Changes in viscoelasticity during the ovulatory menstrual cycle. Fertil. Steril. 28, 47–52.
Yanagimachi, R., 1970. The movement of golden hamster spermatozoa before and after capacitation. J. Reprod. Fertil. 23, 93–196.